Microelectronic Engineering 159 (2016) 42–45

Contents lists available at ScienceDirect

Microelectronic Engineering

journal homepage: www.elsevier.com/locate/mee

Design and fabrication of suspended Si_3N_4 nanobeam cavities

Loukas Athanasekos *, Aristi Christofi, Georgios Gantzounis, Eftychia Bolomyti, George Papageorgiou, Maria-Christina Skoulikidou, Ioannis Raptis, Nikolaos Papanikolaou

Institute of Nanoscience and Nanotechnology, NCSR "Demokritos", GR-153 10 Athens, Greece

ARTICLE INFO

Article history:
Received 23 October 2015
Received in revised form 28 January 2016
Accepted 20 February 2016
Available online 24 February 2016

Keywords:
Silicon nitride nanobeams
Photonic crystals
e-Beam lithography
Suspended nanostructures

ABSTRACT

We report on the design, theoretical simulations and fabrication details of photonic crystal nanobeams (PhCNB) in air-bridge silicon nitride structures. The PhC nanobeams consist of a one-dimensional photonic crystal lattice of circular air holes. The design of structures that show band gaps for the waveguide modes will allow the creation of suspended photonic nanobeam cavities in a second step. The silicon nitride layer is deposited on top of a thermally oxidized silicon wafer with LPCVD followed by e-beam lithography and proper wet etching to release the suspended structures.

1. Introduction

Photonic crystal cavities can confine light in small volumes that lead to strong light-matter interactions and enhance non-linear optical processes and light emission. Photonic crystal nanobeam cavities (PhCNC) in suspended nanobeams perforated with holes have attracted much interest recently, due to the reduced device footprint and their ability to localize light in a narrow wavelength region and achieve high quality factors (Q) in a low mode volume. During the last years, several attempts to study and realize nanobeam cavities have been reported [1–5]. The versatility of this scheme is depicted from the fact that PhCNC have been used in many areas. They have been successfully employed for protein detection [6] and even more complex devices have been developed for biosensing applications [7]. The concept of suspended PhCNC has been also realized in polymer materials for gas sensing [8]. In addition, PhCNC exhibit a great potentiality for optomechanical effects [9–11]. Moreover, the use of slotted PhCNC results in the strong electric field enhancement in the slotted region, enabling strong light-matter interaction [12–14]. Additionally, PhCNC cavities have been successfully employed for the continuous and reversible tuning of the cavity resonance over a 10 nm wavelength range [15]. Furthermore, PhCNC of different geometries have been reported, including H-shaped [16] and ladder-shaped holes [17]. Here we report on the design and fabrication of suspended silicon nitride PhCNC with perforated holes.

2. Photonic band gaps in silicon nitride nanobeams

Before designing cavities, it is essential to control the fabrication of photonic crystals that show frequency regions where no propagation is allowed. Silicon nitride nanobeams periodically perforated with holes are expected to have band gaps for the guided modes. We consider a Si_3N_4 nanowire of width (W) and height (h) perforated with air holes of radius (r). The wire is surrounded with air, and the holes are periodically arranged with a hole-to-hole separation (a). A unit cell of the periodic structure is depicted in Fig. 1 where we also show the planes of mirror symmetry. The behavior of the waveguide can be understood through the calculated dispersion diagram shown in Fig. 2. The simulations were performed using a finite element method implemented in the COMSOL Multiphysics® package. The perforated nanobeam has two symmetry planes one that is normal to the holes, cutting it in two halves, (mirror plane XY) and another one along the periodicity (x-axis) parallel to the z-plane (mirror plane XZ), illustrated in Fig. 1. As a result, guided modes can be classified according to the symmetry of the electric field, as odd or even upon reflection in the mirror planes. In the particular case (W = 400 nm, h = 200 nm, a = 315 nm, r = 60 nm) depicted in Fig. 2a we observe that no absolute gap exists. The black line corresponds to XY-even-XZ-odd modes, with respect to reflections in the first and second mirror planes respectively. Accordingly the blue line is an odd-even, while the red denotes even-even and the green odd-odd modes. The mode profiles at the edges of the Brillouin zone are also shown in the Fig. 2. Band gaps can be optimized since both the size and the middle-gap position are controlled by geometry. In Fig. 2b,c we show band gap maps for the two lower frequency modes for varying hole radius and width of the nanobeam. Small absolute band gaps occur in our structures for smaller width

* Corresponding author.
E-mail address: l.athanasekos@inn.demokritos.gr (L. Athanasekos).

http://dx.doi.org/10.1016/j.mee.2016.02.040
0167-9317/

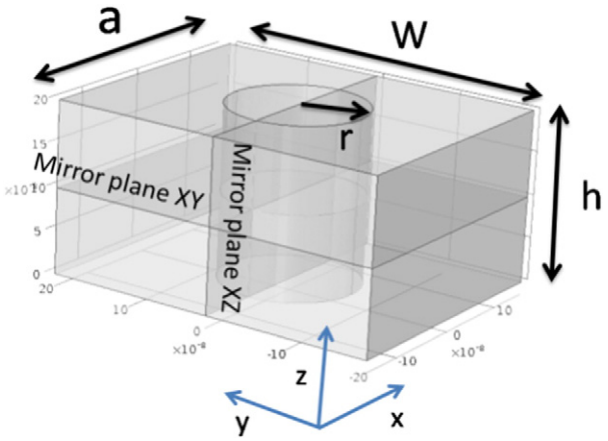

Fig. 1. Schematic of the unit cell, the nanobeam extends in the x direction, symmetry mirror planes parallel to the xy plane (mirror plane XY) and normal to the xy plane (mirror plane XZ) are also shown.

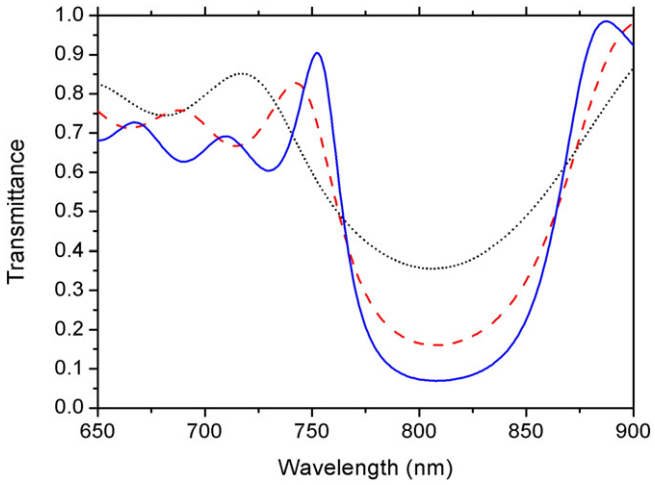

Fig. 3. Calculated transmission spectrum for an even-odd mode of a Si_3N_4 nanobeam (W = 400 nm, h = 200 nm) through a segment perforated with 5 (black dotted line), 7 (red-dashed line), and 9 (blue full line) holes of radius r = 60 nm separated by 315 nm from each other.

and larger hole radii. Adjusting the lattice constant, and wire height offers additional degrees of freedom.

However since it is possible experimentally to excite only the XY-even modes, partial band gaps are of interest, provided that fabrication imperfections are small and no significant mode intermixing occurs due to deviations from the theoretically assumed rectangular shape of the nanobeam. The number of holes required to achieve a good reflecting mirror varies depending on the size of the gap. For a silicon nitride nanobeam in air with W = 400 nm, and h = 200 nm with holes (r = 60 nm) separated by 315 nm we have calculated the transmission spectrum for the lower frequency even-odd modes for varying number of holes. As shown in Fig. 3, for this particular geometry, several holes are required to achieve high reflectivity (low transmission) in the gap region (compare with Fig. 2a, black lines). Our study is the first step towards the design of cavities in the nanobeams that can be realized by introducing a central tapering (variation in the hole size) in the wire between two periodic segments (Bragg mirrors).

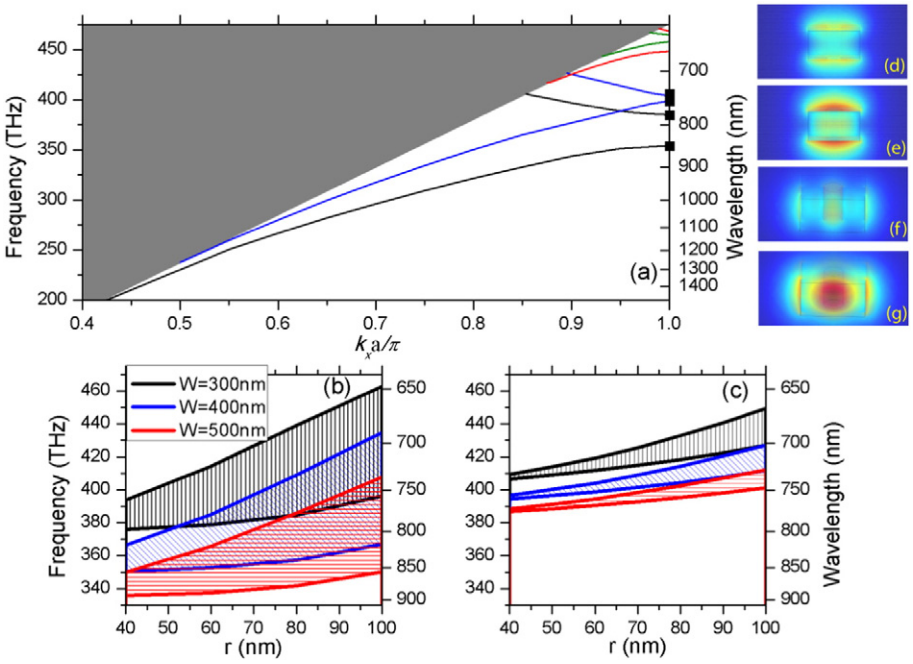

Fig. 2. (a) Dispersion diagram for a Si_3N_4 nanobeam (height h = 200 nm, width W = 400 nm) periodically perforated with air holes (periodicity a = 315 nm, radius r = 60 nm). The gray area marks the region inside the light line that separates the guided modes inside the nanobeam from the free space propagating modes. Different modes are classified according to the symmetry of the electric field. Black line: XY-even, XZ-odd modes, blue line: XY-odd, XZ-even, red line: XY-even, XZ-even, green line: XY-odd, XZ-odd. For a discussion on the different symmetries see text. (b) Variation of the band gap (band gap maps) for the even-odd modes (black curves in (a)) with the width of the nanobeam W and radius of the holes r. Periodicity and height are kept constant (a = 315 nm, h = 200 nm). The shaded areas indicate the size of the band gap for varying radius. (c) The same as (b) but for the odd-even modes, blue curves in (a). (d–g) Mode profiles (normalized absolute value of the electric field) for the four lower frequency modes (d: higher frequency, g: lower frequency) at the edge of the 1D Brillouin zone ($k_x = \pi/a$), indicated with the black squares in (a). A plane normal to the nanobeam direction, between the holes, slightly tilted to allow for perspective, is shown.

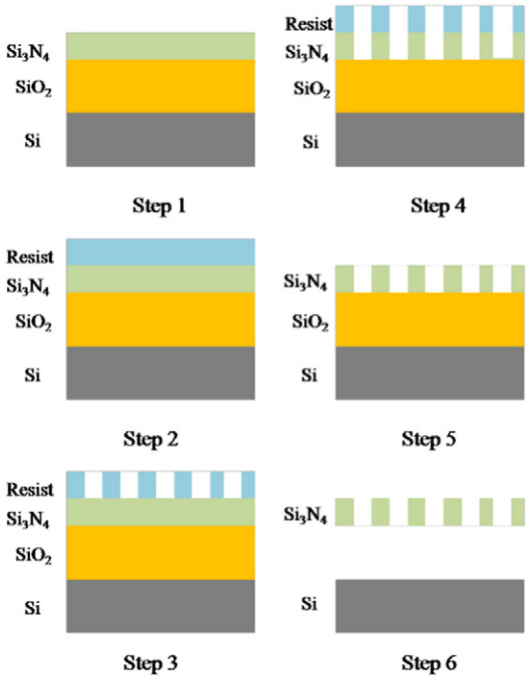

Fig. 4. Fabrication process steps (see text).

3. Fabrication methods

The deposition of silicon nitride is performed on a 3 μm-thick SiO_2 on a silicon substrate (Fig. 4, step 1) with LPCVD. The temperature was set at 800 °C, while the pressure was 23 mTorr. Following a standard CMOS process, we fabricated a 200 nm-thick amorphous Si_3N_4 layer by applying 20 sccm SiH_2Cl_2 and 60 sccm NH_3. The refractive index of the Si_3N_4 was measured with spectroscopic ellipsometry (M2000-F, J.A. Woolam Inc.) and found 2.01. Details on the stoichiometry can be found elsewhere [18]. It should be noted that thicker layers are difficult to obtain due to stress phenomena. For patterning, the sample was first covered with a 380 nm thick AR-N 7520.18 resist. We used a proximity effect correction process to ensure the high fidelity of the fabricated structures as compared to the nominal values. The designed waveguides and nanobeam cavities were then patterned in the resist with a VISTEC EBPG 5000plus 100 kV electron beam lithography system with sub 10 nm resolution, followed by a reactive ion etching (RIE). The waveguides were defined through etching using CHF_3 with 50 sccm flow rate, and pressure 10 mTorr at 400 W power, and frequency 13.5 MHz which delivers a Si_3N_4 etching rate of 36 nm/min (Fig. 4, steps 2–4). The thickness of the fabricated waveguides is measured with laser interferometry, ellipsometry and surface profile meter and all measurements were found in excellent accordance. As a final step, wet etching of the nanocavity region using buffered HF achieving 80 nm/min etching rate for SiO_2, provides the necessary undercut in order to release the structures (Fig. 4, steps 5–6). Prior to dicing, the sample is coated with resist AZ (spin-coat at 3000 rpm for 30 s, followed by bake at 95 °C for 10 min) in order to have a thick layer of 1.65 μm for dicing protection. The edges of the sample are then diced from the back surface (dicing saw Disco DAD-321) which reduces damage of the waveguide edges. The final step comprises the removal of the protective resin by acetone, propanol and PIRANHA 1:1 solution. Finally the samples were dried with nitrogen at low pressure.

The fabricated structures were characterized with a Scanning Electron Microscope (FESEM JEOL JSM 7401F) to evaluate their quality. The final structures are shown in the electron micrograph of Fig. 5a. A typical nanobeam cavity perforated with air-holes is shown in Fig. 5b.

During the initial attempts for the creation the suspended nanobeams, the etching of the underlying SiO_2 layer was a two step process in order to control the etching depth, as depicted in Fig. 5a. The etching depth was 1.6 μm. Moreover, the resulting holes of the cavity were found in good circular shape, with dimensions slightly larger as compared to nominal values, which can be attributed to the BHF etching process. Further optimization of the fabrication process should result in structures with dimensions very close to the designed values.

4. Conclusions

Design, theoretical simulations and fabrication details of photonic crystal nanobeams (PhCNB) in air-bridge silicon nitride structures have been reported. Initial studies have shown promising results, indicating that the nanobeam structures could be an alternative to cavities in 2D photonic crystal slabs. Optimization of the fabrication process will result in the further localization of light in the visible and near infrared region and allowing for, inter alia, information processing, optical modulation, biological and environmental sensing applications. Future attempts will focus on the optical characterization of the structures with regard to quality factors achieved and optimization of the simulation and fabrication process.

Acknowledgments

This work was co-funded by the European Union (ESF) and the Greek state under the ARISTEIA II action (grant number 4709, project THUNDER) of the operational program “Education and lifelong learning”.

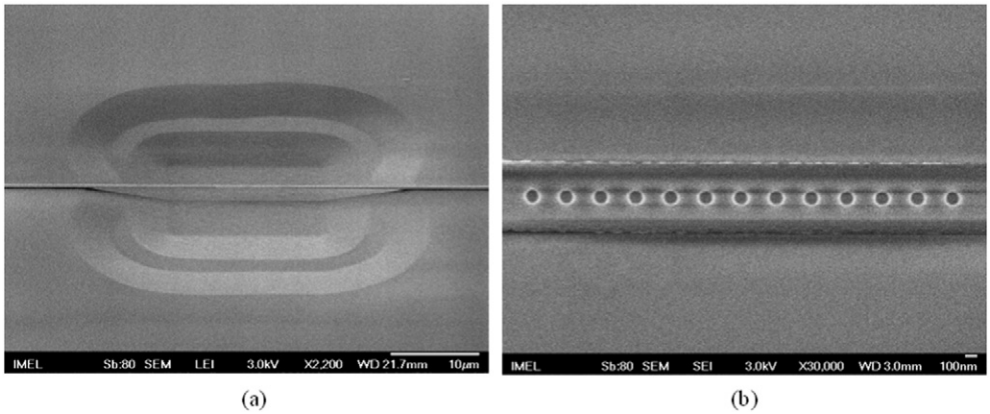

Fig. 5. (a) Panoramic image of the suspended perforated nanobeam. (b) Detail of the nanobeam with perforated holes.

References

[1] M. Khan, T. Babinec, M.W. McCutcheon, P. Deotare, M. Loncar, Fabrication and characterization of high-quality-factor silicon nitride nanobeam cavities, Opt. Lett. 36 (3) (2011) 421–423.

[2] P.B. Deotare, M.W. McCutcheon, I.W. Frank, M. Khan, M. Loncar, High quality factor photonic crystal nanobeam cavities, Appl. Phys. Lett. 94 (2009) 121106.

[3] P.B. Deotare, M.W. McCutcheon, I.W. Frank, M. Khan, M. Loncar, Coupled photonic crystal nanobeam cavities, Appl. Phys. Lett. 95 (2009) 031102.

[4] J.D. Ryckman, S.M. Weiss, Low mode volume slotted photonic crystal single nanobeam cavity, Appl. Phys. Lett. 101 (2012) 071104.

[5] Q. Quan, P.B. Deotare, M. Loncar, Photonic crystal nanobeam cavity strongly coupled to the feeding waveguide, Appl. Phys. Lett. 96 (2010) 203102.

[6] F. Liang, N. Clarke, P. Patel, M. Loncar, Q. Quan, Scalable photonic crystal chips for high sensitivity protein detection, Opt. Express 21 (2013) 32306.

[7] Q. Liua, X. Tua, et al., Highly sensitive Mach–Zehnder interferometer biosensor based on silicon nitride slot waveguide, Sensors Actuators B Chem. 188 (2013) 681–688.

[8] H. Clevenson, P. Desjardins, X. Gan, D. Englund, High sensitivity gas sensor based on high-Q suspended polymer photonic crystal nanocavity, Appl. Phys. Lett. 104 (2014) 241108.

[9] D. Ramos, I.W. Frank, P.B. Deotare, I. Bulu, M. Loncar, Non-linear mixing in coupled photonic crystal nanobeam cavities due to cross-coupling opto-mechanical mechanisms, Appl. Phys. Lett. 105 (2014) 18.

[10] Y. Li, et al., Optomechanical crystal nanobeam cavity with high optomechanical coupling rate, J. Opt. 17 (2015) 045001.

[11] M. Davanc, et al., Slot-mode-coupled optomechanical crystals, Opt. Express 20 (22) (2012) 24394.

[12] S. Lin, J. Hu, L. Kimerling, K. Crozier, Design of Nanoslotted Photonic Crystal Waveguide Cavities for Single Nanoparticle Trapping, Proc. OSA/CLEO/IQEC, 2009.

[13] P. Seidler, K. Lister, U. Drechsler, J. Hofrichter, T. Stöferle, Slotted photonic crystal nanobeam cavity with an ultrahigh quality factor-to-mode volume ratio, Opt. Express 21 (26) (2013) 32468–32483.

[14] P. Xu, K. Yao, J. Zheng, X.i Guan, Y. Shi, Slotted photonic crystal nanobeam cavity with parabolic modulated width stack for refractive index sensing, Opt. Express 21 (22) (2013) 26908.

[15] I.W. Frank, P.B. Deotare, M.W. McCutcheon, M. Loncar, Programmable photonic crystal nanobeam cavities, Opt. Express 18 (8) (2010) 8705.

[16] C. Deng, H. Peng, Y. Gao, J. Zhong, Ultrahigh-Q photonic crystal nanobeam cavities with H-shaped holes, Phys. E. 63 (2014) 8–13.

[17] Y. Gong, et al., Observation of transparency of erbium-doped silicon nitride in photonic crystal nanobeam cavities, Opt. Express 18 (13) (2010) 13863.

[18] X. Guo, T.P. Ma, Tunneling leakage current in oxynitride: dependence on oxygen/nitrogen content, IEEE Electron Device Lett. 19 (6) (1998).